A High-Efficiency Single-Phase Grid-Tied Inverter Featuring Reactive Power Support

SHAIK AYESHA BEGUM [1] | DR D.SIVA PRASAD[2]

[1]Pg Scholar, Dept of EPS, Kodada Institute of Technology & Science for Women-Kodad, Telangana.

[2] Assistant Professor, Dept of EEE, Kodada Institute of Technology & Science for Women-Kodad,Telangana.

ABSTRACT: Photovoltaic (PV) solar power is one of the most promising renewable energy sources. Compared to off-grid solutions, grid-integrated solar power is far more widely used. For grid-tied applications, removing transformers can lower the overall system weight and cost. However, when there is no galvanic isolation between an ac grid and PV, a leakage current with a large peak value passes through the system. Furthermore, future grid-tied systems need to guarantee reactive power injection. In order to lower the root mean square (RMS) and peak value of leakage current, the authors of this work have suggested a new hybrid architecture that uses both decoupling and mid-point clamping techniques. Furthermore, the grid can receive both active and reactive electricity from the suggested architecture. The Matlab/Simulink environment is used to simulate the topology under both open loop and closed loop situations. The leakage current issue has been resolved under open loop conditions. Model predictive control (MPC) is used to inject active power (P) and reactive power (Q) into the grid under closed loop conditions. Lastly, a comparison with other comparable topologies has been carried out.

KEYWORDS: PV, MPC, RMS, ACTIVE POWER, REACTIVE POWER.

I.INTRODUCTION: Renewable energy options are seen to have promise for reducing the need of fossil fuel-based energy sources. There is no other way to reduce CO2 emissions without using renewable energy. On the other hand, because solar energy is widely available and environmentally friendly, it is both clean and global. An inverter is used to convert the dc power from solar cells into ac power. There are two methods for using solar energy: ON grid and OFF grid. Compared to the OFF grid system, the ON-grid system is far more widely used [1]. ON grid systems use an inverter with or without a transformer to inject solar energy into an ac grid. When a transformer is employed, galvanic isolation is created between the solar photovoltaic system and an ac grid [2], [3], [4], [5], which helps to improve the system's common mode issues. However, efficiency declines and the whole system weight rises. The issues with an inverter with a transformer can be mitigated in the case of a transformerless inverter. Furthermore, an industrial option for low-voltage applications is a single-phase transformerless inverter.

Because transformerless inverter systems lack galvanic isolation, a greater leakage current may flow, potentially introducing harmonics and electromagnetic interference into the grid current [7, 8, 9]. All of these elements elevate the possibility of safety issues including electric shock and increase grid current ripple [7, 8, 9]. The safety issues may become more serious if the leakage current unexpectedly peaks. Table 1 illustrates the VDE 0126-1-1 standard [10] pertaining to the inverter's common mode behavior. Furthermore, not every topology works well for adding reactive power (Q) to an ac grid. However, in grid-tied applications, this control is necessary for future voltage regulation [11], [12].

TABLE 1. VDE 0126-1-1 standard [10].

RMS Leakage Current (mA)	The Time of Disconnection (s)
100	0.04
60	0.15
30	0.3

Decoupling and mid-point clamping techniques have been used to solve leakage current issues because of their improved THD performance and ease of design and implementation. Numerous single-phase transformerless inverter topologies have been developed in the literature to reduce leakage current. The authors reduced leakage current by using the dc decoupling technique in the zero-voltage state. Nevertheless, neither the leakage current nor its unwanted peak can be eliminated. Even if the topologies suggested are appropriate for injecting reactive power (Q) into the grid, the authors did not conduct an experiment to confirm this. The topologies are unable to supply the grid with Q. The authors used the ac decoupling technique to remove the leakage current, but they merely decreased the leakage current's rms value rather than its peak. is unable to supply Q, nevertheless. To lower the leakage current during the freewheeling phase, the mid-point clamping approach was used. They are unable to completely eliminate the leakage current, though. The sudden peak of the leakage current cannot be eliminated by mid-point clamped topologies. Although the author did not conduct an experiment to support their assertion, the topology can be used to supply Q to the grid. Using an R-L load rather than a direct grid, the authors demonstrated the reactive power capabilities of their suggested topology. Q cannot be injected into the grid via Reference. In order to solve the aforementioned issues, the authors proposed a few different topologies.

II.PROPOSED SYSTEM: In order to minimize leakage current and preserve Q flow, the authors suggested a hybrid architecture that combines mid-point clamping and decoupling approaches. The paper's primary contributions are: to suggest a new hybrid architecture for the grid that has lower peak and rms leakage current values and Q capabilities. Additionally, to demonstrate that the suggested architecture may inject Q into the grid, a model predictive control is used.

A. SUGGESTED TOPOLOGY The recommended topology is shown in Fig. 1. Zero-kingdom DC decoupling, zero-kingdom AC decoupling, and zero-kingdom mid-point clamping strategies form the foundation of this topology. This topology makes use of nine switches. While S7 became used for mid-factor clamping, S5 and S6 have been hired for AC decoupling. DC decoupling became accomplished the usage of S8 and S9. Two same-fee enter DC hyperlink capacitors were linked in collection. One filter out capacitor and two same-price inductors were used as filter out inductors..

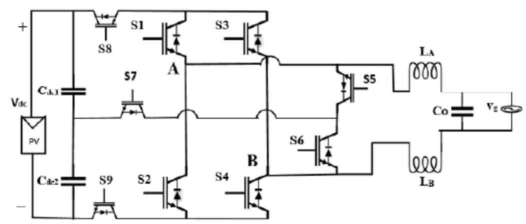

FIGURE 1. Proposed topology.

B. OPERATING MODES

1) WHEN POWER FACTOR =1 The switching states of the various modes of the counseled topology with a trailing strength factor are shown in Table 2. Both nice and bad electricity areas are present in a half of cycle. The operating modes under non-solidarity electricity factor are depicted in Fig. 2. The voltage and present day waveforms with lagging pf are shown in Fig. 3. There are eight distinct methods of operation to be had right here. When S8 and S9 are activated and the grid voltage and contemporary are high quality, Mode 1 takes place. The system enters mode 2 whilst S8 and S9 are off and the grid voltage and modern are advantageous in the fine 1/2-

cycle. When S8 and S9 are both in mode 3, the grid voltage is fantastic but the grid current is bad during the high quality half-cycle. Mode 4 occurs whilst S8 and S9 are off because the grid voltage is wonderful however the grid current is negative during the wonderful half of-cycle. When the grid voltage and modern are bad, S8 and S9 perform in mode 5. The system enters mode 6 while S8 and S9 are off and the grid voltage and current are terrible during the terrible half of-cycle. The grid voltage is negative at the same time as S8 and S9 are both on, however the grid current is effective at some stage in the poor half of-cycle; this is known as mode 7. In mode 8, S8 and S9 are off, yet the grid voltage is poor and the grid modern is high quality.

TABLE 2. Switching states of different modes of the proposed topology with a lagging power factor.

Grid voltage	Power	Mode	S1	S2	S3	S4	S5	S6	S7	S8	S9
positive	positive	mode 1	1	0	0	1	1	0	0	1	1
positive	positive	mode 2	0	0	0	0	1	1	1	0	0
positive	negative	mode 3	1	0	0	1	1	0	0	1	1
positive	negative	mode 4	0	0	0	0	1	1	1	0	0
negative	positive	mode 5	0	1	1	0	0	1	0	1	1
negative	positive	mode 6	0	0	0	0	1	1	1	0	0
negative	negative	mode 7	0	1	1	0	0	1	0	1	1
negative	negative	mode 8	0	0	0	0	1	1	1	0	0

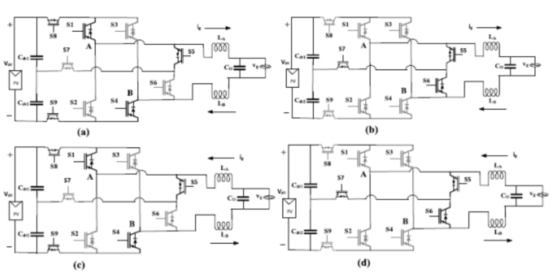

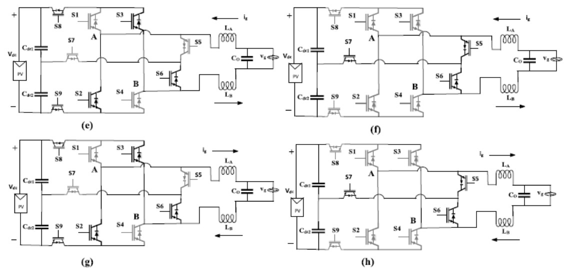

FIGURE 2. Operating modes when pf ≠1 (a) mode 1 (b) mode 2 (c) mode 3 (d) mode 4 (e) mode 5 (f) mode 6 (g) mode 7 (h) mode 8.

The grid current in this situation could either lead or lag the grid voltage. The grid can receive both reactive power (Q) and active power (P) from the inverter. The Q injection will determine how much the grid current is trailing or leading.

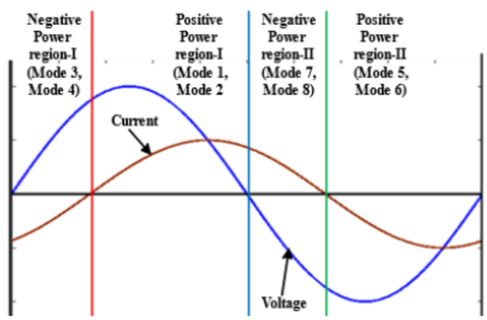

FIGURE 3. Voltage and current waveforms with lagging pf.

This research analyzes the Q injection capacity of the proposed inverter using simply lagged pf. The maximum Q injection will depend on the system's maximum current rating. The following are the formulas for total common mode voltage, or VtCM, in various modes: For active modes 1 and 3, which are positive half cycles:

$$V_{tCM} = \frac{V_{AN} + V_{BN}}{2} = \frac{V_{dc} + 0}{2} = \frac{V_{dc}}{2} \quad (1)$$

For negative half cycle active modes (mode 5 and mode 7):

$$V_{tCM} = \frac{V_{AN} + V_{BN}}{2} = \frac{0 + V_{dc}}{2} = \frac{V_{dc}}{2} \quad (2)$$

For freewheeling modes (mode 2, mode 4, mode 6 and mode 8):

$$V_{tCM} = \frac{V_{AN} + V_{BN}}{2} = \frac{\frac{V_{dc}}{2} + \frac{V_{dc}}{2}}{2} = \frac{V_{dc}}{2} \quad (3)$$

2) WHEN POWER FACTOR = 1 There are simplest fantastic strength regions in this instance. When the grid voltage is going through a tremendous 1/2 cycle, modes 1 and a pair of of Fig. 2 may be present. The modes 5 and 6 depicted in Fig. 2 will take location while the grid voltage is inside the bad 1/2 cycle. A. MANAGEMENT METHODS The topology and grid have been linked via the use of Model Predictive Control (MPC). The advised grid-based totally manage approach is proven in Fig. Four. Leakage contemporary is unaffected by the maximum electricity factor monitoring (MPPT) controller that the dc-dc converter makes use of to offer the dc reference voltage. The output of the DC-DC converter will seem like a brief circuit due to the high frequency leakage modern. Thus, the leakage current will only pass via impartial. For this motive, DC voltage has taken the placement of PV as the inverter's input. Vdc is the voltage throughout the dc link capacitors. This regulation permits the grid to get the desired energetic and reactive electricity. The inverter voltage and current previous to the filter are denoted via vi and ii, respectively. The symbols vg and ig stand for the grid voltage and contemporary, respectively. The α and β components of vg and ig are created the use of Matlab/Simulink's discrete variable time delay (DVTD) block with a purpose to put into effect the control strategies with the dSpace 1104 controller. In order for MPC to generate the specified pulses for the inverter, reference current and forecast modern are generated as follows: The perceived strength of the reference,

$$S_{ref} = P_{ref} + JQ_{ref} = v_g i^*_{gref} \quad (4)$$

where,

$$v_g = v_{g\alpha} + jv_{g\beta} \quad (5)$$

And,

$$i_{gref} = i_{g\alpha ref} + ji_{g\beta ref} \quad (6)$$

The full expression for the grid current is,

$$i_g = i_{g\alpha} + ji_{g\beta} \quad (7)$$

The real component of i_{gref} is expressed as,

$$i_{g\alpha ref} = \left(P_{ref} v_{g\alpha} + Q_{ref} v_{g\beta}\right) \Big/ \left(v_{g\alpha}^2 + v_{g\beta}^2\right) \quad (8)$$

The imaginary component of i_{gref} is expressed as,

$$i_{g\beta ref} = \left(-Q_{ref} v_{g\alpha} + P_{ref} v_{g\beta}\right) \Big/ \left(v_{g\alpha}^2 + v_{g\beta}^2\right) \quad (9)$$

Model Predictive Control is used to write the expected current at the (k +1)th iteration for various vi(k) states as follows:

$$i_g(k+1) = \left(1 - \frac{RT_S}{L}\right) i_g(k) + \frac{T_S}{L}\left(v_i(k) - v_g(k)\right) \quad (10)$$

where L stands for filter inductance, R is the filter inductors' series resistance, TS is the sampling time, and vi (k) is the inverter output voltage prior to filtering. This is how the cost function is calculated:

$$Cost\ function,\ g = \left| i_{gref}(k) - i_g\,(k+1) \right| \qquad (11)$$

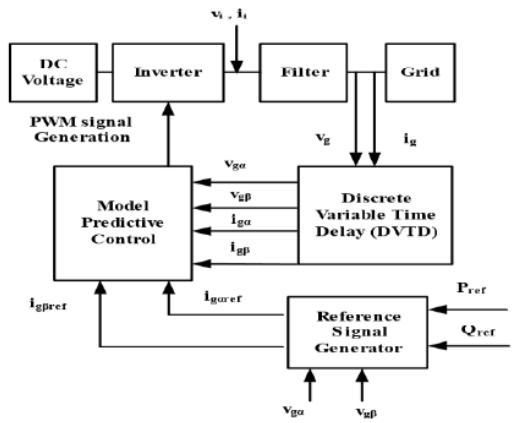

FIGURE 4. Control scheme for the proposed topology with grid.

Where L stands for filter out inductance, R is the filter out inductors' series resistance, TS is the sampling time, and vi (ok) is the inverter output voltage prior to filtering. This is how the fee feature is calculated. In the cautioned topology, complete bridge switches are used to get the vital cost of vi (okay), and in addition switches are used to finish the method for coping with the leakage current troubles. Finally, this PWM is carried out to the proposed inverter. B. MODULATION METHODS For the recommended inverter, there are two techniques for generating the unipolar PWM pulses: an open loop approach and a closed loop technique. When the output voltage is 0, S8 and S9 are first deactivated, starting the DC decoupling methods. Second, even as conducting AC decoupling during freewheeling levels, S5 and S6 offer an additional freewheeling route. In order to hold a regular overall not unusual mode voltage, S7 also compresses the mid-factor voltage underneath zero voltage occasions. By the usage of all of those techniques, the suggested topology is able to permit reactive electricity waft whilst lowering the peak and RMS values of leakage current.

1) MODULATION FOR OPEN LOOP The pulse generating technique below open loop situations (with resistive load) is shown in Fig. Five. Fig. 6 displays the switching pulses for the recommended structure. The switching frequency of the S8 and S9 switches is whole cycle. S7 features on switching frequency at some point of its entire cycle, just like S8 and S9, but inside the opposite manner. Only the effective half-cycle is used to prompt S1 and S4 at switching frequency. The S6 switching sample is the reverse of the S4 and S1 patterns. It operates on switching frequency during the nice 1/2-cycle and grid frequency at some stage in the poor half of-cycle. Only the negative half of-cycle is used to function S2 and S3 at switching frequency. S5 uses grid frequency in the superb half of-cycle

and switching frequency in the poor 1/2-cycle.

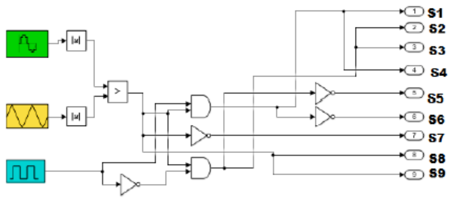

FIGURE 5. Modulation technique of the proposed topology for open loop.

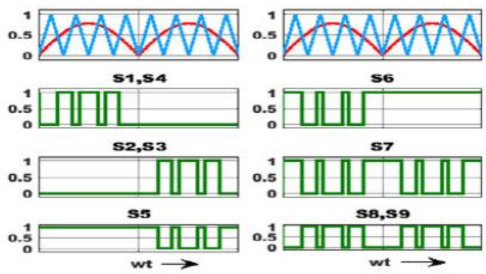

FIGURE 6. Switching pulses of the proposed topology for open loop.

III.SIMULATION RESULTS:

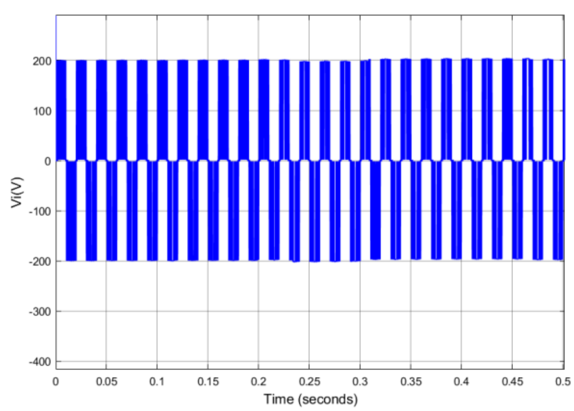

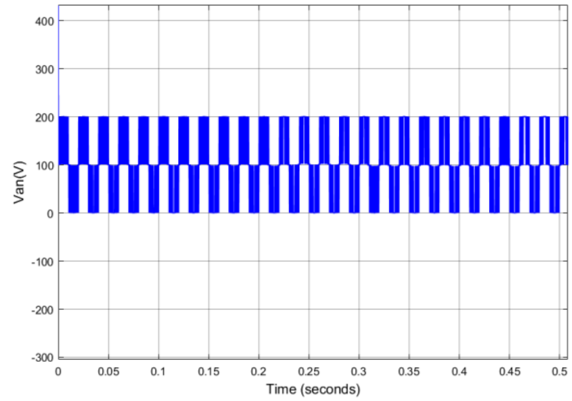

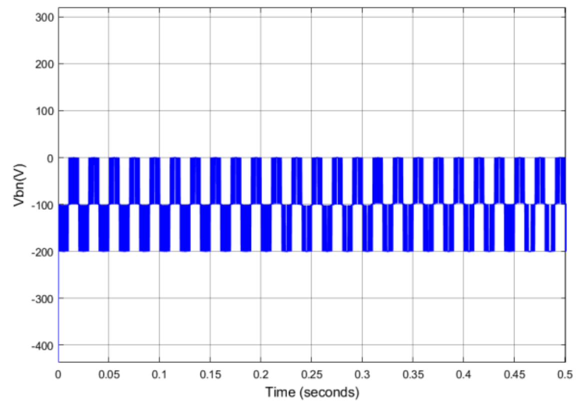

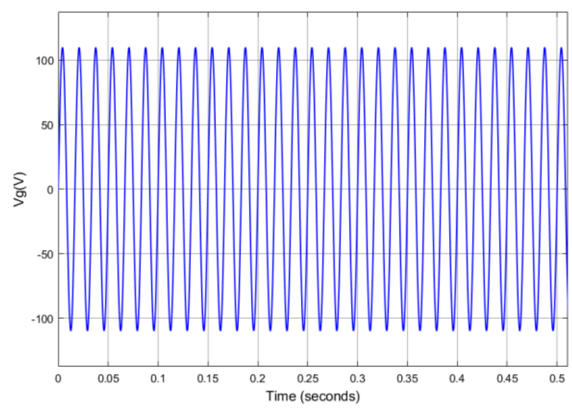

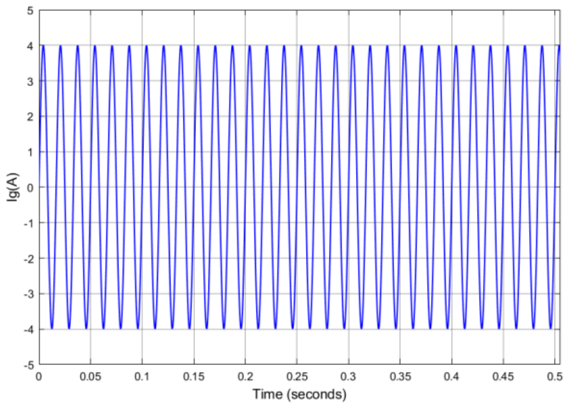

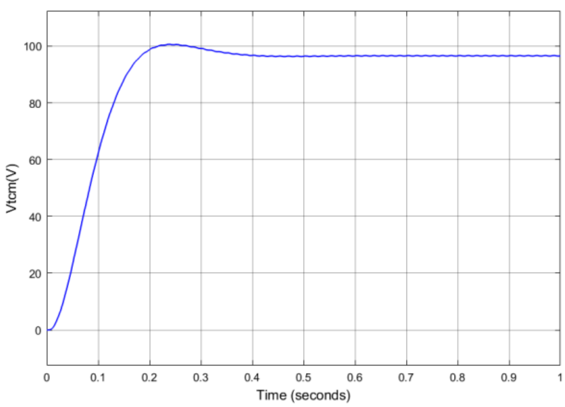

IV.CONCLUSION: This paper introduces a novel hybrid topology based on mid-point clamping and decoupling. To lower leakage current and enable reactive power injection into the grid, the benefits of decoupling and mid-point clamping approaches have been combined. The leakage current generated by the suggested inverter does not appear to peak. The suggested inverter can maintain a reduced leakage current (peak=5 mA, rms=2.85 mA) at 110V AC. Open loop simulations and experiments have been used to show how well the suggested inverter performs in terms of leakage current. In addition, P and Q can be injected into the grid via the suggested inverter. Through closed loop models and experiments, this reactive power capability has been confirmed using a direct grid and model predictive control. The THD performance is likewise excellent at just 1.1% when compared to other current topologies. All of the aforementioned benefits have been realized by utilizing a few additional switches. In the future, single phase transformerless low voltage photovoltaic applications can use this inverter with more safety and dependability.

REFERENCES: [1] Int. Energy Agency. (2024). PVPS Trends Report 2024. [Online]. Available: https://www.iea-pvps.org

[2] M. N. H. Khan, Y. P. Siwakoti, M. J. Scott, L. Li, S. A. Khan, D. D. Lu, R. Barzegarkhoo, F. Sidorski, F. Blaabjerg, and S. U. Hasan, ‘‘A common grounded type dual-mode five-level transformerless inverter for photovoltaic applications,’’ IEEE Trans. Ind. Electron., vol. 68, no. 10, pp. 9742–9754, Oct. 2021, doi: 10.1109/TIE.2020.3028810.

[3] M. Islam and S. Mekhilef, ‘‘An improved transformerless grid connected photovoltaic inverter with reduced leakage current,’’ Energy Convers. Manage., vol. 88,

pp. 854–862, Dec. 2014, doi: 10.1016/j.enconman.2014.09.014.

[4] H. Xiao, ‘‘Overview of transformerless photovoltaic grid-connected inverters,’’ IEEE Trans. Power Electron., vol. 36, no. 1, pp. 533–548, Jan. 2021, doi: 10.1109/TPEL.2020.3003721.

[5] X. Zhao, D. Jiang, J. Chen, Z. Shen, and Q. Li, ‘‘Leakage current suppression with capacitor voltage control of three-level flying capacitor grid-connected inverters,’’ IEEE Trans. Ind. Electron., vol. 69, no. 3, pp. 2191–2201, Mar. 2022.

[6] S. V. Araujo, P. Zacharias, and R. Mallwitz, ‘‘Highly efficient single phase transformerless inverters for grid-connected photovoltaic systems,’’ IEEE Trans. Ind. Electron., vol. 57, no. 9, pp. 3118–3128, Sep. 2010, doi: 10.1109/TIE.2009.2037654.

[7] Ó. López, F. D. Freijedo, A. G. Yepes, P. Fernández-Comesaña, J. Malvar, R. Teodorescu, and J. Doval-Gandoy, ‘‘Eliminating ground current in a transformerless photovoltaic application,’’ IEEE Trans. Energy Convers., vol. 25, no. 1, pp. 140–147, Mar. 2010, doi: 10.1109/TEC.2009.2037810.

[8] M. Bahrami-Fard, N. Moeini, M. Shahabadini, H. Iman-Eini, and M. Liserre, ‘‘A new topology and modulation strategy to suppress the leakage current in transformerless cascaded H-bridge inverters in PV application,’’ IEEE J. Emerg. Sel. Topics Power Electron., vol. 11, no. 1, pp. 1219–1229, Feb. 2023. [Online]. Available: https://ieeexplore.ieee.org/document/9732476/

[9] H. K. Jahan, ‘‘A new transformerless inverter with leakage current limiting and voltage boosting capabilities for grid-connected PV applications,’’ IEEE Trans. Ind. Electron., vol. 67, no. 12, pp. 10542–10551, Dec. 2020, doi: 10.1109/TIE.2019.2960728.

[10] Eigenerzeugungsanlagen Am Niederspannungsnetz, document VDE V0126-1-1, 2006.

[11] B. Liu, M. Su, J. Yang, D. Song, D. He, and S. Song, ‘‘Combined reactive power injection modulation and grid current distortion improvement approach for H6 transformer-less photovoltaic inverter,’’ IEEE Trans. Energy Convers., vol. 32, no. 4,

pp. 1456–1467, Dec. 2017, doi: 10.1109/TEC.2017.2712741.

[12] T. K. S. Freddy, J.-H. Lee, H.-C. Moon, K.-B. Lee, and N. A. Rahim, ‘‘Modulation technique for single-phase transformerless photovoltaic inverters with reactive power capability,’’ IEEE Trans. Ind. Electron., vol. 64, no. 9, pp. 6989–6999, Sep. 2017, doi: 10.1109/TIE.2017.2686366.